Bollettino di Geofisica Teorica ed Applicata Vol. 56, n. 3, pp. 407-424; September 2015
DOI 10.4430/bgta0154

Optimizing the automatic location of the real-time Antelope® system in north-eastern Italy

L. Moratto and D. Sandron

Istituto Nazionale di Oceanografia e di Geofisica Sperimentale (OGS), Centro Ricerche Sismologiche, Trieste and Udine, Italy

(Received: January 13, 2015; accepted: June 15, 2015)

ABSTRACT North-eastern Italy is one of the most seismically active areas of Italy, being affected in the past by eight destructive earthquakes. This area is densely populated and heavily industrialized, hence its seismic monitoring is crucial for Civil Defense purposes. This task is managed by the Istituto Nazionale di Oceanografia e di Geofisica Sperimentale (OGS), through its Centro Ricerche Sismologiche (CRS), that performs the automatic real-time locations through the Antelope® BRTT software package. An accurate choice of the Antelope® setting parameters is necessary to ensure the best performance of the real-time system, that means the most accurate location for the earthquakes with magnitude $M_L \geq 2.5$ (the alarm threshold), avoiding any false event. This goal was pursued by testing different parameters on a data set built with 295 earthquakes representative of the local seismicity. The tuned parameters were then validated on the earthquakes which occurred in the monitored area in 2011: all events with $M_L \geq 2.5$ were correctly detected and located with a median epicentral distance difference of 2 km with respect to the OGS catalogue. The OGS real-time system was tuned with these parameters that have been operating successfully since 2012.

Key words: north-eastern Italy, automatic location, seismic monitoring, Emilia, Antelope®.

1. Introduction

North-eastern Italy, with the nearby regions of Austria, Slovenia and Croatia, corresponds to the northernmost part of the Adriatic microplate which in this sector collides and rotates anti-clockwise with respect to the Eurasian plate (Carulli and Slejko, 2005). The movement induces a remarkable state of stress. As a consequence the area and in particular the pre-Alpine belt from Lake Garda to the Italian-Slovenian border is one of the most seismically active districts of Italy (Slejko *et al.*, 1989). The Italian earthquake catalogue CPTI11 (Rovida *et al.*, 2011) reports 8 destructive earthquakes (with macroseismic epicentre $I_0 \geq$IX MCS) in this sector and the most recent is the quake of May 6, 1976 (Carulli and Slejko, 2005) that caused 989 casualties and stimulated the beginning of detailed seismological studies in north-eastern Italy. The space distribution of the epicentres (Fig. 1) describes well the pre-Alpine piedmont belt with the main concentration in central Friuli and to a lesser extent around Lake Garda. Moving to the

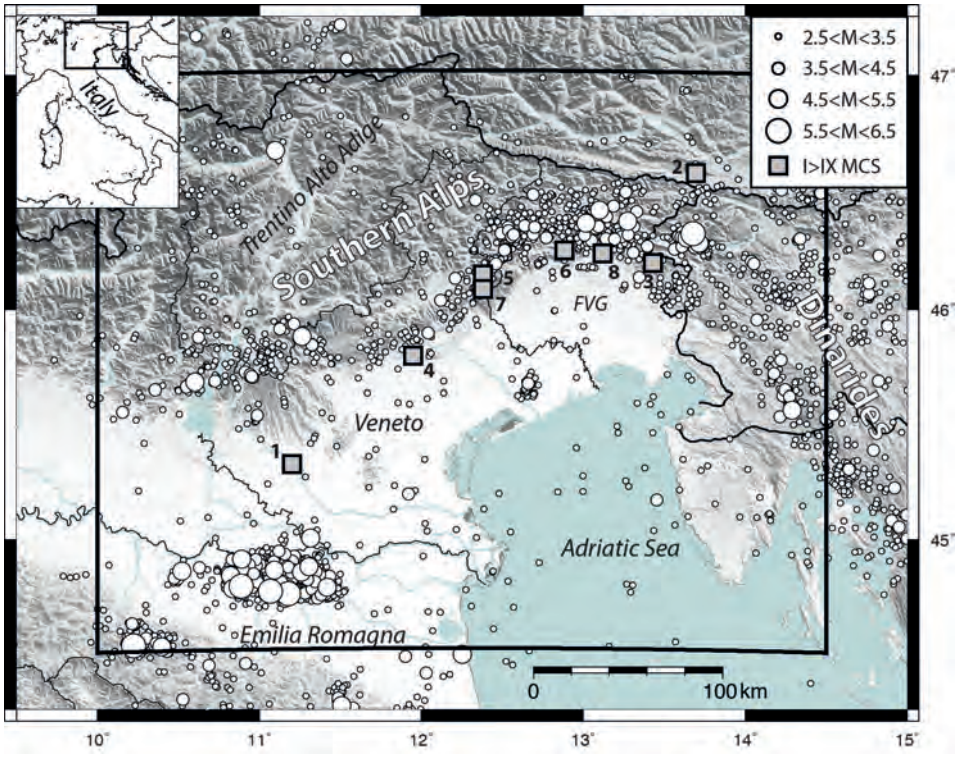

Fig. 1 - Map of the seismicity in the north-eastern Italy: the circles show the locations of the seismic events occurred in the period 1977-2013 and retrieved from the OGS bulletin while the squares represent the epicentres of earthquakes with an I_0 greater than IV MCS from 1000 A.D. to May 5, 1977 from the CPTI catalogue (Rovida *et al.*, 2011). The main events are: 1) 1117 Veronese, 2) 1348 Carinzia, 3) 1511 Slovenia, 4) 1695 Asolano, 5) 1873 Bellunese, 6) 1928 Carnia, 7) 1936 Bosco Cansiglio, 8) 1976 Friuli. The black box represents the NEI area monitored by OGS.

east, the epicentres are more spread over most of Slovenia with a more defined NW-SE trend along the Croatian coast. The Database of Individual Seismogenic Sources (DISS) (Basili *et al.*, 2008; DISS Working Group, 2010) reports the main active composite seismogenic faults that are schematized as boxes (Fig. 2). The orogenic belt of the Southern Alps is composed of closely spaced, generally south-verging overthrusts, while the Dinaric system is characterized by overthrusts and by mostly dextral, sub-vertical faults with direction ranging between NW-SE and NNW-SSE (Slejko *et al.*, 1989). North-eastern Italy, in particular in the aforementioned pre-Alpine belt, has a high seismic hazard, with an expected maximum acceleration for an exceedance probability of 10% in 50 years between 0.250 and 0.275 g (Gruppo di Lavoro MPS, 2004). Recently the Emilia earthquake sequence of 2012 also evidences the presence of significant seismicity in the Po Plain involving the frontal sector of the northern Apennines, and in particular the buried front of the Emilia north-verging active thrust belt (Fantoni and Franciosi, 2010).

The scientific institution deputed for the earthquake monitoring in north-eastern Italy is the Istituto Nazionale di Oceanografia e di Geofisica Sperimentale (OGS), through its Centro Ricerche Sismologiche (CRS) and its seismic network (Fig. 2), that integrates the regional seismic networks of Friuli Venezia Giulia (FVG) and Veneto regions as well as that of Trentino, managed by the Provincia Autonoma di Trento (Garbin and Priolo, 2013). At present the OGS

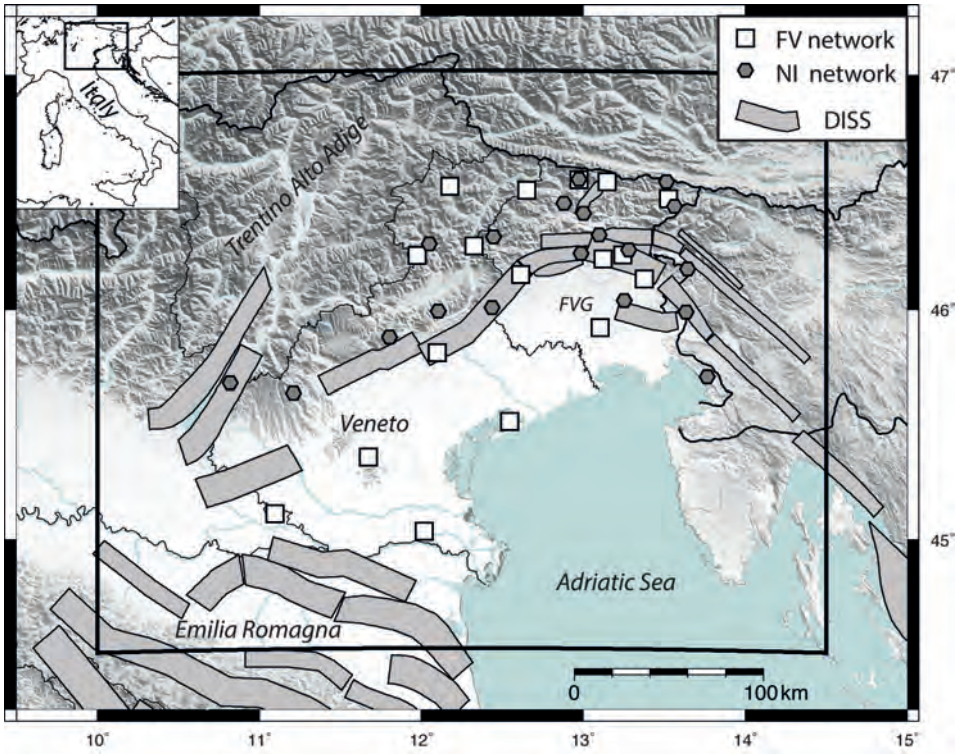

Fig. 2 - The OGS stations operating in the north-eastern Italy. The hexagons represent broad-band stations of the NI network (Table 1) while the squares show the short-period stations of the FV network (Table 2). The boxes are the composite seismogenic sources taken from the Database of Individual Seismogenic Sources (DISS Working Group, 2010).

network comprises 35 stations deployed in an area stretching from Lake Garda in the west to the Italian-Slovenian border in the east, and from the River Po in the south to the Italian-Austrian border in the north (Fig. 2, Tables 1 and 2). The seismic signals are acquired and processed in real-time by the Antelope® software (Bragato *et al*., 2011a) from Boulder Real-Time Technologies (BRTT); the software is installed on a Mac Pro machine equipped with a processor Quad-Core Intel Xeon (the speed is 2.66 GHz), the RAID volumes and Mac OS X. The Antelope® system also manages the real-time data exchange in the Southern Alps area with the Zentralanstalt fur Meteorologie und Geodynamik (ZAMG) in Austria, the Agencija Republike Slovenije za Okolje (ARSO) in Slovenia, the University of Trieste (UNITS), the Istituto Nazionale di Geofisica e Vulcanologia (INGV) and the Swiss Seismological Service (SED) (Table 3). The sharing of cross-border waveforms improves the actual network geometries and, as a consequence the earthquake detection threshold near the borders. The real-time data exchange strongly increases the number of recording stations acquired in the OGS data centre and nowadays more than 100 stations are used to locate the seismic events. The Antelope® locations are immediately sent to the local civil protection headquarters and uploaded to the related web pages (http://rts.crs.inogs.it) where the annual bulletin of seismicity (Priolo *et al*., 2005) reporting locations, magnitudes and picking data according to the HYPO71 standard (Lee and Lahr, 1975) is published. The analysis on the complete catalogue evidences

that the completeness magnitude is equal to 1.5 (Gentili *et al*., 2011) in FVG region, the median horizontal and vertical uncertainties are 3.4 km (95% within 11 km) and 4.2 km (95% within 16 km) respectively and the median root-mean-square (rms) traveltime residual is equal to 0.8 s (95% within 1.4 s) (Sandron, 2011).

Table 1 - Broadband stations operated by OGS, their geographic location and instrumentations; these stations belong to NI network (north-eastern Italy broadband seismic network).

Code	Name	Lat. °N	Lon. °E	Alt. (m)	Lithography	Digitizer	Broad band instrument	Accelerometer instrument
ACOM	Acomizza	46°32′55″	13°30′53″	1715	limestone	Q330	STS-2	Episensor
AGOR†	Agordo	46°16′56″	12°02′50″	631	limestone dolostone	Gaia	STS-2	Episensor
BALD	M. Baldo	45°40′59″	10°49′08″	1911	olitic limestone	Q330	Trillium-40	Episensor
BOO	Bordano	46°19′11″	13°05′55″	444	limestone	Q330	Trillium-120	Episensor
CAE	Caneva	46°00′31″	12°26′17″	870	limestone	Q330	Trillium-120	----------
CGRP	C. Grappa	45°52′50″	11°48′17″	1757	limestone	Q330	STS-2	Episensor
CIMO	Cimolais	46°18′41″	12°26′41″	610	dolomitic limestone	Q4120	STS-2	Episensor
CLUD	Cludinicco	46°27′25″	12°52′53″	635	limestone	Q330	Trillium-120	Episensor
DRE	Drenchia	46°10′24″	13°38′42″	810	marly sandstone	Q330	Trillium-40	Episensor
FUSE	Fusea	46°24′51″	13°00′04″	520	schlern dolostone	Q330	Trillium-40	Episensor
MARN	Marana	45°38′16″	11°12′36″	785	basalts	Q330	Trillium-40	Episensor
MPRI	M. Prat	46°14′26″	12°59′14″	762	limestone	Q330	Trillium-40	Episensor
PRED	Cave Predil	46°26′34″	13°33′54″	902	dolostone	Q330HR	STS-2	Episensor
SABO	M. Sabotino	45°59′15″	13°38′01″	621	limestone	Q330	STS-2	Episensor
VARN	Col Varnada	45°59′36″	12°06′17″	870	limestone	Q330	Trillium-120	Episensor
VINO§	Villanova	45°15′21″	13°16′52″	608	limestone	Q4120	CMG-3T	Episensor
ZOU2	Zouf Plan	46°33′30″	12°58′22″	1911	dolostone	Q330	Trillium-120	Episensor
TRI*	Trieste	45°42′32″	13°45′51″	161	limestone	Q4120	STS-1	----------

† AGOR is managed in collaboration with INGV
§ VINO is managed in collaboration with the University of Trieste
* TRI is managed in collaboration with the University of Trieste and INGV

Due to OGS institutional role and to ensure an optimal service and best efficiency, the aim of this study is the optimization of the real-time system regarding the algorithms that detect and locate the earthquakes in the monitored area of north-eastern Italy (NEI) evidenced in Fig. 1 (black box). This means setting the software parameters in order to recognize and to estimate in a preliminary and automatic way the location of all the seismic events with magnitude larger than the alarm threshold ($M_L \geq 2.5$), avoiding any false event. This issue is fundamental to guarantee reliable and consistent results and each network operator should tune his location system adopting a methodology similar to the approach described in this study. Different parameter combinations were tested on a data set made up of 295 earthquakes recorded in the last years and representative (in terms of magnitude range and geographical distribution) of the studied area seismicity. We validate the best parameters setup performing the procedure on the date recorded in 2011. A similar study was undertaken by Garbin and Priolo (2013) limited to the Trentino area and focused only on a semiautomatic offline procedure which is useful to analyze the microseismicity of the area and thus not able to perform the real-time alert for civil defense purposes.

2. Real-time parameter setup

Antelope® is a system of software modules developed for real-time seismic acquisition, automated detection, processing (e.g., picking, association, location, magnitude estimation) and data storage. This study is focused on the algorithms (detection and the association modules) that recognize and locate the seismic event; we used the version 5.2 of Antelope®. The short-term average crosses through a long-term average (STA/LTA) algorithm defines the detection threshold and it is applied with different bandpass filters on the continuous waveforms. These frequency ranges are strictly related with the characteristics of the signal contents for local (high frequency range), regional (intermediate frequency range) and teleseismic earthquakes (low frequency range); if a trigger threshold is exceeded, the detection is declared open, tabulated on the Antelope® database, and it will be closed when the STA/LTA ratio becomes lower than a de-trigger threshold. These detections are matched to estimate origin time computed on a 3D grid of nodes with a fixed-velocity model. Different filters in the detection correspond to different 3D spatial grids utilized in the association. For example the local events require the detection at higher frequencies and a search grid set up on a local area with an adequate resolution. After the detection process, all of the times in the pick list are reduced by the phase travel times to an equivalent origin time and the standard association search is performed on all grids looking for a single solution that produces the most numbers of defining P-arrivals within the specified cluster time window. The declaration of the earthquake is set by the minimum number of triggered stations and the time window to associate the phases, that is a crucial parameter and it must be finely tuned. The solution obtained by the 'trial-and-error' association on the 3D grids is used as the starting solution in order to perform the GENLOC inversion (Pavlis *et al.*, 2004) and to obtain a stable earthquake location. The GENLOC library (Pavlis *et al.*, 2004) uses the Gauss-Newton method (Lee and Stewart, 1981) proposed by Geiger (1910) and which is similar to the HYPOELLIPSE algorithm (Klein, 1978).

Table 2 - Short-period seismic stations operated by OGS, their geographic position and instrumentations; these stations belong to FV network (Friuli Venezia Giulia and Veneto regional short-period network).

Code	Name	Lat. °N	Lon. °E	Alt. (m)	Lithography	Instrumentation
ADRI	Adria	45°02'16''	12°01'00''	1	alluvial sediments	Lenn. Le3DLite
AFL	A. Faloria	46°31'42''	12°10'42''	2235	dolostone	Lenn. Le3DLite
BAD	Bernadia	46°14'03''	13°14'36''	590	limestone	Lenn. Le3DLite
BUA	Buia	46°13'00''	13°07'25''	320	flysch	Lenn. Le3DLite
COLI	Colloredo	46°07'56''	13°22'36''	250	flysch	Lenn. Le3DLite
CSM	C. Mimoias	46°30'44''	12°39'07''	1640	sandstone	Lenn. Le3DLite
CSO	Casso	46°16'24''	12°19'26''	1070	limestone	Lenn. Le3DLite
FAU	F. Aurine	46°13'56''	11°58'31''	1430	schists	Lenn. Le3DLite
GAZZ	Gazzo V.	45°06'48''	11°05'42''	12	alluvial sediments	Lenn. Le3DLite
IESO	Jesolo	45°31'04''	12°32'47''	0	sand	Lenn. Le3DLite
LSR	Lussari	46°28'30''	13°31'38''	1750	-	Lenn. Le3DLite
MLN	Malnisio	46°09'00''	12°36'53''	814	limestone	Lenn. Le3DLite
MTLO	Montello	45°48'48''	12°05'48''	350	molasse	Lenn. Le3DLite
PLRO	Paularo	46°32'56''	13°08'53''	1420	diabase	Lenn. Le3DLite
TEOL	Teolo	45°21'42''	11°40'26''	370	marls	Lenn. Le3DLite
TLI	Talmassons	45°55'15''	13°06'12''	-74	alluvial sediments	Mark L4C
ZOU	Zoufplan	46°33'27''	12°58'26''	1896	dolostone	Lenn. Le3DLite

In a first stage, the different parameters were tested on a selected data set (hereafter DBALL) to reduce the computation time. This data set contains a restricted number of earthquakes selected to be representative of the average seismicity of the studied area both in the distribution of epicentre locations and in magnitude range. Thus 295 earthquakes have been chosen from the NEI bulletin related to years 2010 to 2012 (Fig. 3) and the local magnitude ranges between 0.2 and 5.0 while the hypocentral depth varies between 0.4 and 30 km. The selected earthquakes refer to about 40 days of recordings representing the seismological characteristics of the NEI area as the seismicity in the piedmont belt within the Veneto and FVG regions, the western Slovenia and the Po Plain zone. Moderate earthquakes located in the Tosco-Emiliano Apennines (ISIDe Working Group, 2010) at SW and SE of the monitored area have been added because the propagation effects in the Po Plain (Bragato *et al*., 2011b) can also make these events felt by the population at relevant distances. Furthermore, these earthquakes allowed us to test the system capabilities for automatically locating events at the border or outside the NEI/OGS network area of confidence because the experience tell us that the seismic events occurring at the NEI border can be critical for our automatic locations.

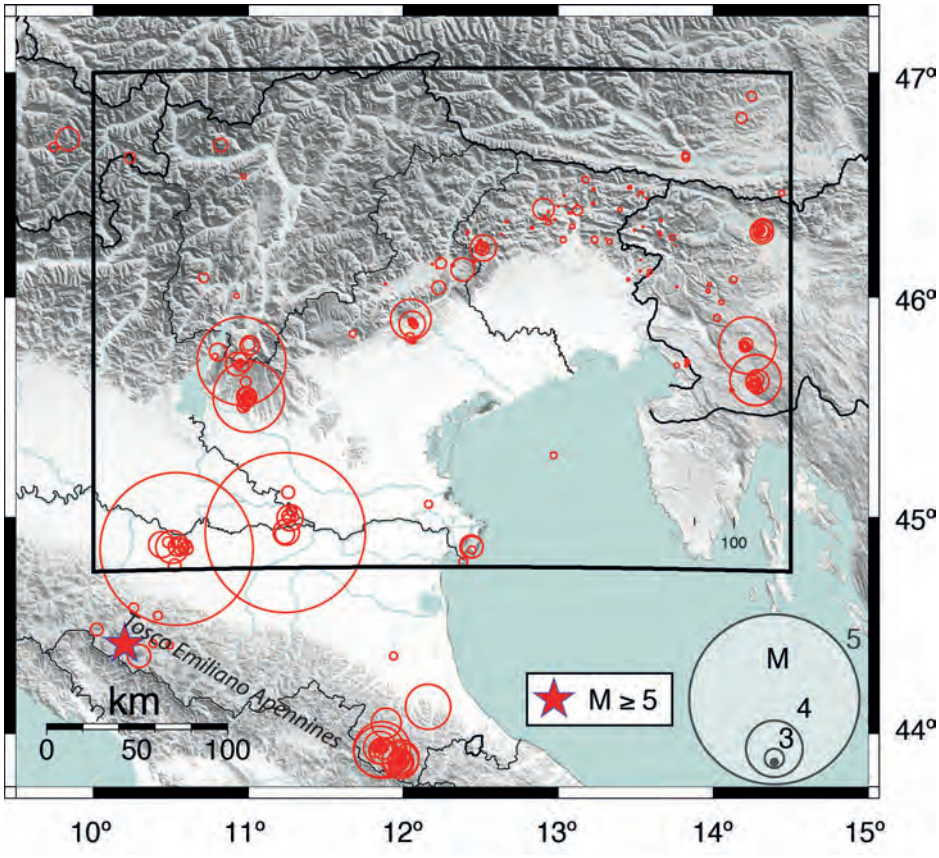

Fig. 3 - The earthquakes of the data set (DBALL) utilized to perform the tests on the Antelope® configuration; DBLOC is constituted by the seismic events located within the black box representing the OGS monitored area

Table 3 - The characteristics of the utilized seismic networks: the network code, the full name description, the management and the number of stations (N) acquired by the OGS Antelope® system. The details of the acquired stations can be found at http://rts.crs.inogs.it/en/project/1_map.html.

Code	Full name	Management	N
CH	Switzerland seismological network	SED	6
FV	Friuli Venezia Giulia and Veneto regional short period networks	OGS	16
IV	Italian national seismic network	INGV	9
MN	Mediterranenan network - MEDNET	INGV	5
NI	North-east Italy regional broad band seismic network	OGS*	28
OE	Austrian seismic network	ZAMG	10
RF	Friuli Venezia Giulia accelerometric network	UNITS	1
SI	Südtirol	Südtirol (Italy)	7
SL	Slovenia seismic network	ARSO	12
ST	Trentino seismic network	Trentino (Italy)	8

* In collaboration with UNITS

The comparison between our results and the epicentral locations published in the OGS bulletins (Priolo *et al*., 2005) is the benchmark of our analysis; this bulletin is the best available reference of the local seismicity in the NEI area because the events are manually located with the signals recorded by all cross-border networks. Two different indicators have been considered to evaluate the goodness of fit: the median value of the difference of the epicentral locations (in km, MDE hereafter) and the percentage ratio of the earthquakes recognized by our system. Further, the confidence bounds of the acceptable solutions are determined by performing the F-test on a null hypothesis as proposed by Mayeda *et al*. (1992) and Bianco *et al*. (2002) on grid search parameters. Once fixed the degrees of freedom, the Fisher distribution related to the indicator ratio is tabulated for each confidence levels: in particular, a selected model is significantly different from the best solution only if the ratio between the single indicator (the MDE value in this case) and the minimum indicator falls outside the confidence level determined by the F-distribution. The F-test on null hypothesis estimates statistically the level of significance of different configuration parameters referred to the best-selected model; practically, a parameter model will be significant different and, therefore, worse, if falls outside the bound representing the confidence level extracted from the Fisher distribution. To obtain a more accurate estimation of the uncertainties and the sensitivity of the models, in this study we compare our results with two confidence levels at 60% and 90%. The same parameters are computed for a restricted data set (hereafter DBLOC) containing only the earthquakes located inside the NEI area in order to evaluate the influence of the events placed inside and outside of the network on the tested models (Fig. 3).

The parameters were settled in three sequential steps connected with the Antelope® procedure: the detection, the grid association, and the GENLOC inversion. In the detection step, we modified the frequency ranges for local, regional, and teleseismic events in order to obtain the best configuration that would be able to identify the single earthquake in the proper grid. Once the best detection parameters were selected, the association configurations were tuned to vary the minimum threshold of associated stations, the uncertainty on the grid associator and the location weights. In the final step several velocity models were tested on the GENLOC algorithm and at the same time different weight configurations were evaluated. The best configuration obtained on the restricted data sets was validated on all data acquired in 2011 in NE Italy. Further two stress tests are made on the 2011 recordings in order to verify the robustness and the stability of our final configuration because we are interested to check the system in case of lack of recordings or a malfunctioning in the data broadcasting.

3. Results

The parameters have been tuned in three different but linked steps in accordance with the Antelope® procedure: the detection, the grid association and the GENLOC inversion performed on DBALL and DBLOC databases.

3.1. Detection

The detection parameters are mainly related to the selection of different frequency ranges in computing the signal to noise ratio (SNR). Furthermore, these frequency ranges are strongly

correlated with the definition of the association grids which must be settled by considering the spatial, geometry of the recording stations. Three different grids have been selected for local, regional, and teleseismic events and the local grid concerns a more extended NEI area, the regional grid overlays Europe and Mediterranean areas while the teleseismic grid refers to other earthquakes. The travel times have been computed for each path between the recording stations and the grid nodes, adopting the standard IASPEI velocity model (Kennett, 1991). The local grid nodes have a horizontal spacing length of 4.0 km (comparable with the horizontal uncertainty in the NEI bulletin: 95% of the 2011 localizations have an epicentral uncertainty less than, or equal to, 3.6 km) while the vertical spacing length is variable and it increases in the deeper layers. We tested nine different settings (Table 4) and the time windows for the ratio of the short and long-term averages are defined separately for the three different detections (local, regional, and teleseismic) while the trigger-on and trigger-off SNR thresholds are fixed respectively at 5.0 and 2.5 for all cases (see Table 5). The definition of the time interval within which the detection is active is very important in order to detect the complete sequence in case multiple events occur within a few seconds away from each other. Antelope® does not allow the opening of a new detection (and the recognition of a possible new earthquake) if an old detection is still open. Since we are interested in recognizing as many earthquakes as possible at the local (and partially regional) scale, these parameters have been settled in a different way for each considered grid (see Table 5). Other parameters that refer to minimum and maximum data sample values are not considered.

Table 4 - Detection parameter models setup. Local, regional, and teleseismic: the filters applied to the waveforms for the local, regional, and teleseismic grids. DBLOC and DBALL: the percentages of the recognized earthquakes in comparison with the published events limited to the DBLOC and the DBALL data set respectively. BP refers to Butterworth bandpass filter, HP to Butterworth highpass filter (see Table 5 for the explanation of various detection parameters).

Model	Local (Hz)	Regional(Hz)	Teleseismic (Hz)	% DBLOC	% DBALL
D1	HP 3.0	BP 2.0-3.0	BP 0.8-2.0	47.8873	37.2881
D2	HP 5.0	BP 3.0-5.0	BP 0.8-3.0	57.7465	57.6271
D3	HP 4.0	BP 3.0-4.0	BP 0.8-3.0	49.2958	54.9153
D4	HP 6.0	BP 3.0-6.0	BP 0.8-3.0	50.7042	50.5085
D5	HP 5.0	BP 4.0-5.0	BP 0.8-4.0	57.7465	45.0847
D6	HP 5.0	BP 2.0-5.0	BP 0.8-2.0	57.7465	49.8305
D7	HP 4.5	BP 4.0-4.5	BP 0.8-4.0	52.1127	48.1356
D8	BP 5.0-25.0	BP 3.0-5.0	BP 0.8-3.0	68.5841	64.7458
D9	BP 5.0-30.0	BP 3.0-5.0	BP 0.8-3.0	66.3717	62.7119

Table 5 - Description of the detection parameters used in the Antelope® system; the best results are in the last columns (model D8 of Table 4) and were obtained for the local, regional, and teleseismic events. BP refers to Butterworth bandpass filter.

Parameter	Description	Local	Regional	Teleseismic
sta_twin	short term average time window	1.0	1.0	2.0
sta_tmin	short term average minimum time for average	1.0	1.0	2.0
sta_maxtgap	short term average maximum time gap	0.5	0.5	0.5
lta_twin	long term average time window	10.0	10.0	20.0
lta_tmin	long term average minimum time for average	5.0	5.0	10.0
lta_maxtgap	long term average maximum time gap	4.0	4.0	4.0
nodet_twin	no detection if on time is less than this	2.0	5.0	10.0
thresh	detection SNR threshold	5.0	5.0	5.0
threshoff	detection-off SNR threshold	2.5	2.5	2.5
det_tmin	detection minimum on time	5.0	10.0	20.0
det_tmax	detection maximum on time	10.0	200.0	600.0
latency	input packet pipe latency in packets	3	3	3
filter	Butteworth filter applied to the signals	BP 5.0-25.0	BP 3.0-5.0	BP 0.8-3.0
iphase	phase code for detection	L	R	G

In the nine tests (listed as D1 to D9 in Table 4) we modified the frequency range for local, regional, and teleseismic events to obtain the best set of parameters in order to detect the single earthquakes in the appropriate grid (e.g., associate the phases of local events with the local grid and so on), leaving the association parameters fixed as default. The teleseismic detection has the cutoff minimum frequency fixed to 0.8 Hz, while the regional detection has been tested on variable ranges with the cutoff minimum frequency varying between 2 and 4 Hz and the cutoff maximum frequency between 4 and 6 Hz (Table 4). At the same time the local detection has been performed with a highpass (HP) or bandpass (BP) filter (tests D8 and D9). The results show that the best configuration has the regional detection ranging between 3-5 Hz (test D2) with about 58% of earthquakes being recognized. With the maximum cutoff frequency fixed at 25 Hz (test D8) in the local detection, the system improves the performance with the recognition of a large number of earthquakes (about 65.0% of all dataset and 68.5% of local events). It is noteworthy that in test D8 all earthquakes with $M_L \geq 2.5$ (the alarm threshold) are correctly detected by the Antelope® procedure.

3.2. Grid association

After fixing the detection parameters of test D8, 20 additional association configurations (Table 6) were tested on the parameters described in Table 7. The declaration of the earthquake is set by the minimum number of triggered stations and the time window to associate the phases. We set the main detection processing window ('process_time_window' parameter) to 500 s,

Table 6 - Grid association parameter models setup. Station threshold: minimum allowable number of stations to locate an earthquake, this parameter depends from maximum source-receiver distance (in degrees) in tests A11÷20. The weights can be applied with different procedures: the source-receiver distance function (DN is the maximum source-receiver distance with weight=1) or the station density radius (SR) or utilizing only the closest stations (CS) to each source node. All distances for various weights are expressed in degrees. Time window: the length of the clustering time window. These parameters can be applied to local (L) and regional (R) associations. MDE: the median value of the difference of the epicentral locations values and the percentages of the associated earthquakes in comparison with the events from the DBLOC and DBALL datasets (see Table 7 for the explanation of various association parameters).

Model	Stations threshold	Weights	Time window (s)	MDE DBLOC (km)	MDE DBALL (km)	DBLOC (%)	DBALL (%)
A1	6	no	L->1.5	2.3691	2.9147	68.5841	64.7458
A2	6	no	L->2.0	2.4867	3.1299	68.1416	62.7119
A3	6	no	L->1.0	2.4315	2.9758	67.5412	62.1186
A4	6	no	R->3.0	2.3691	3.0254	68.1856	61.8644
A5	6	L -> CS=30	L->1.5	2.4626	3.0046	68.5841	64.4068
A6	6	L -> DN=0.5°	L->1.5	2.4854	3.1299	68.5841	64.7458
A7	6	L -> DN=1.0°	L->1.5	2.3938	2.9830	68.5841	63.0508
A8	6	L -> SR=0.1°	L->1.5	2.3966	3.0901	68.5841	64.7458
A9	6	R -> SR=0.1°	L->1.5	2.3691	2.9361	68.5841	65.0847
A10	6	R -> SR=0.2°	L->1.5	2.3691	2.9547	68.5841	64.7458
A11	4 (d≤0.1°) 6 (d≤0.5°) 8 (d≤1.0°) 10 (d≤180°)	no	L->1.5	2.3297	2.8962	61.9469	58.9831
A12	4 (d≤0.5°) 6 (d≤1.5°) 10 (d≤180°)	no	L->1.5	2.3356	2.8749	71.8938	68.8136
A13	4 (d≤0.5°) 6 (d≤0.8°) 8 (d≤1.0°) 10 (d≤180°)	no	L->1.5	2.2765	2.7910	67.6991	63.3898
A14	4 (d≤0.5°) 6 (d≤1.5°) 8 (d≤2.0°) 10 (d≤180°)	no	L->1.5	2.2516	2.7793	72.5664	69.1525
A15	4 (d≤0.5°) 6 (d≤1.5°) 8 (d≤2.0°) 10 (d≤180°)	L -> DN=0.5°	L->1.5	2.4151	2.9161	72.5664	69.1525
A16	4 (d≤0.5°) 6 (d≤1.5°) 8 (d≤2.0°) 10 (d≤180°)	L -> SR=0.1°	L->1.5	2.4499	3.0485	72.5664	69.1525
A17	4 (d≤0.5°) 6 (d≤1.5°) 8 (d≤2.0°) 10 (d≤180°)	R -> SR=0.1°	L->1.5	2.3804	2.9133	72.5664	69.1525
A18	4 (d≤0.5°) 6 (d≤1.5°) 8 (d≤2.0°) 10 (d≤180°)	R -> SR=0.4°	L->1.5	2.3804	2.9133	72.5664	69.1525
A19	4 (d≤0.5°) 6 (d≤1.5°) 8 (d≤2.0°) 10 (d≤180°)	R -> SR=0.6°	L->1.5	2.4779	2.9391	72.5664	69.1525
A20	4 (d≤0.5°) 6 (d≤1.5°) 8 (d≤2.0°) 10 (d≤180°)	R L-> CS=30°	L->1.5	2.3748	2.9215	72.5664	69.1525

Table 7 - Description of the association parameters used in the Antelope® system; the best results are in the last columns (model A14 of Table 6) and were obtained for the local, regional, and teleseismic events.

Parameter	Description	Local	Regional	Teleseismic
nsta_thresh	minimum allowable number of stations to locate an earthquake; in case of local events this parameter is expressed as a function of maximum source-receiver distance in degrees	4 for d≤0.4° 6 for d≤1.5° 8 for d≤2.0° 10 for d≤180°	10	14
nxd	number of east-west grid nodes for depth scans	11	11	----
nyd	number of north-south grid nodes for depth scans	11	11	----
cluster_twin	clustering time window in seconds that is used to determine whether an observed arrival associates with a hypothetical event location	1.5	2.0	5.0
try_S	also S travel-times are tried to locate the events	no	no	no
phase_sifter	detection phase code used in association	L	R	G
priority	priority to select the association in case of locations falling inside multiple grids	3	2	1
use_dwt	use source receiver distance weighting factor	no	no	no
dwt_dist_near - DN	if use_dwt=yes, the maximum source-receiver distance with weight=1	-	-	-
sta_weight_radius - SR	a radius in degrees that is used to compute a station density weighting factor used to weight picks from each station	no	no	no
closest_stations - CS	use only a selected number of closest stations to a particular source node in the search for defining phases	no	no	no
relocate	run the relocation script (inversion) to refine the final solution	yes	no	no

because this parameter must correspond to the total phase moveout time difference between the closest and the furthest node distances; the detection list is processed each time 20 new detections are imported from the table ('process_ncycle' parameter). We changed the minimum number of phases to locate a local earthquake (this value is fixed to 10 for regional events and 14 for teleseismic events), the clustering time window ('cluster_twin' parameter in Table 7) and the weights configuration. The clustering time window has been set to 1.5 s for local and 2.0 s for regional earthquakes starting from test A5 (other values gave worse results on DBALL data set events). A relevant improvement in defining associations (more than 70% of DBLOC events) was given by the adoption of the minimum phases depending upon the maximum source-receiver distance in degrees (tests A11-A20). This is used to define the low number-of-stations solutions only in the case where the available stations are relatively close to the event. Small changes of this parameter produces significant changes in MDE values that decrease from 2.91 to 2.78 km (from 2.37 to 2.25 km on DBLOC, from test A1 to test A14) recognizing about 72% of local earthquakes. In the grid association the weights can be parameterized in a different way [in Table 7: 'dwt_Dist_Near' (DN), 'Sta_weight_Radius' (SR) and 'Closest_Stations' (CS)], with their definitions depending on the source-receiver distance (DN in tests A6, A7

and A15), from a radius in degrees used to compute a station density weighting factor (SR in tests A8-A10 and A16-A19) and from including only the closest stations to each source node (CS in tests A6 and A20). These tests show that the adoption of different configurations in the weights definition does not improve the performance system, but it causes a general worsening due to the uneven distribution of the recording stations and the lack of instruments in some grid zones. After our tests, the best model results the set of parameters adopted in test A14. The F-test evidences that the MDE values differ significantly with a confidence level of 90% in all considered cases of DBALL and DBLOC except test A13; in this case the confidence level is limited to 60% but the percentage of earthquakes located is strongly lower than the best model.

3.3 GENLOC inversion

As the final step different velocity models were tested on the GENLOC inversion algorithm (Pavlis *et al*., 2004), keeping fixed the parameters of the D8 model for the detection and the A14 model for the grid association. At the same time, some different configurations were evaluated with the weights factor depending on the source-receiver distance (see Table 7). We tested a global velocity model, IASPEI (Kennett, 1991), and two velocity models defined for the FVG region and the Slovenia area (Bressan, 2005), named Friuli and Slovenia respectively; the velocity models (Table 8) are quite simple with only three (IASPEI and Friuli) or four layers (Slovenia). The tests G1-G3 (Table 9) show that the difference can be relevant (the MDE value ranges between 2.10 and 2.23 km for local events) and the model Friuli gives the best results. The test on the weights indicates the model G4 as the best: in this case the weights decrease linearly with the increment of the source-receiver distance. A comparison between the starting model D1 with the final model G4 allows us to appreciate the efficacity of the new parameters selection: the events detection increases from 37% to 69% (from 48% to 72% for DBLOC events) and the MDE value decreases from 2.91 to 2.31 km (from 2.37 to 2.07 km for DBLOC events). All earthquakes with the magnitude value equal to, or larger than, the alarm threshold are correctly recognized and located. The F-test indicates that the adoption of different velocity models gives MDE values differing significantly with a confidence level of 90%; in the case of the tests G4-G7 the confidence level is limited to 60%. We remember that the GENLOC inversion assumes as starting model the results obtained from the grid association which means that the inversion can improve the starting grid result but the GENLOC algorithm cannot adjust a starting location which is totally wrong.

Table 8 - P-wave velocity as a function of depth (H) for Friuli (FRI), Slovenia (SLO) and IASPEI models.

H (km)	Vp (km/s)		
	FRI	SLO	IASPEI
0	5.85	5.9	5.8
9		6.4	
20			6.5
22	6.8	6.7	
35			8.0
39.5	8.0		
40		8.0	

Table 9 - 'GENLOC' inversion model setup. Weights: the weights applying the source-receiver distance function (DN is the maximum source-receiver distance in degrees with weight=1). MDE: the median value of the difference of the epicentral locations values in comparison with the events from the DBLOC and DBALL data sets (see Table 7 for the explanation of various inversion parameters).

Model	Velocity model	Weight	MDE DBLOC	MDE DBALL
G1	Friuli	none	2.1033	2.4387
G2	Slovenia	none	2.1635	2.5416
G3	IASPEI	none	2.2293	2.5951
G4	Friuli	DN=0.0°	2.0674	2.3097
G5	Friuli	DN=0.5°	2.0701	2.3552
G6	Friuli	DN=1.0°	2.0842	2.3657
G7	Friuli	DN=1.5°	2.0904	2.3851

3.4. Validation

The final system configuration (model G4) was validated by applying the procedure used on the 2011 recordings. The results were compared with the locations published in the OGS bulletin. 67% of the events listed in the 2011 bulletin are recognized and located with a MDE equal to 2.04 km (Fig. 4); this value decreases to 1.64 km in the case of earthquakes which occurred within the OGS network, where 74% of the earthquakes are detected. The median of the difference between the hypocentral depths is 3.6 km which is reduced to 3.2 km only if the local earthquakes are considered.

All events with the magnitude value equal to, or larger than, the alarm threshold are correctly recognized and located (Fig. 4). In particular we locate all events with the magnitude values larger than 1.5 in FVG, Austria and Slovenia areas, while this value increases to 2.0 in Veneto and to 2.5 in other bordering zones. The spatial density of the recording stations and the related level of background noise influence strongly the sensibility of the detections and the capacity of locating also the microseismicity, both for real-time alert purposes and in the production of the bulletin.

3.5 Stress tests

Two stress tests have been done to check the robustness of the system in case of lack of recordings due to a hypothetic broadcast crash and the consequently unavailability of short period data and the case of lack of the extra-OGS networks contributing. In the first test we did not use the OGS short period data (see Table 2) that are transmitted by radio and acquired later respect to the other stations. The first automatic location is usually done without the short period recordings and it is interesting to evaluate the weight of this "latecomer" signals on the locations. The comparison between the locations obtained in this way and these of the 2011 bulletin shows that MDE increases to 2.48 km (2.06 km for local events) and the percentage of located events decreased to 51% (58% for local data set). We locate all events with magnitude larger than 1.9 in FVG and 2.3 in Veneto (Fig. 4). In the second test we supposed a broadcast block with other data centres so only the OGS data are available (see Tables 1 and 2); the comparison between our locations with the 2011 bulletin data shows that the MDE value remains unchanged but the percentage of the recognized events decreased strongly to 38%, with the largest part of lost events located outside or at the border of the NEI area (Fig. 4). The magnitude completeness does not exceed the alarm threshold and all earthquakes with the magnitude larger than 1.5 in FVG and 2.0 in Veneto are recognized, but this value increases in the bordering zones.

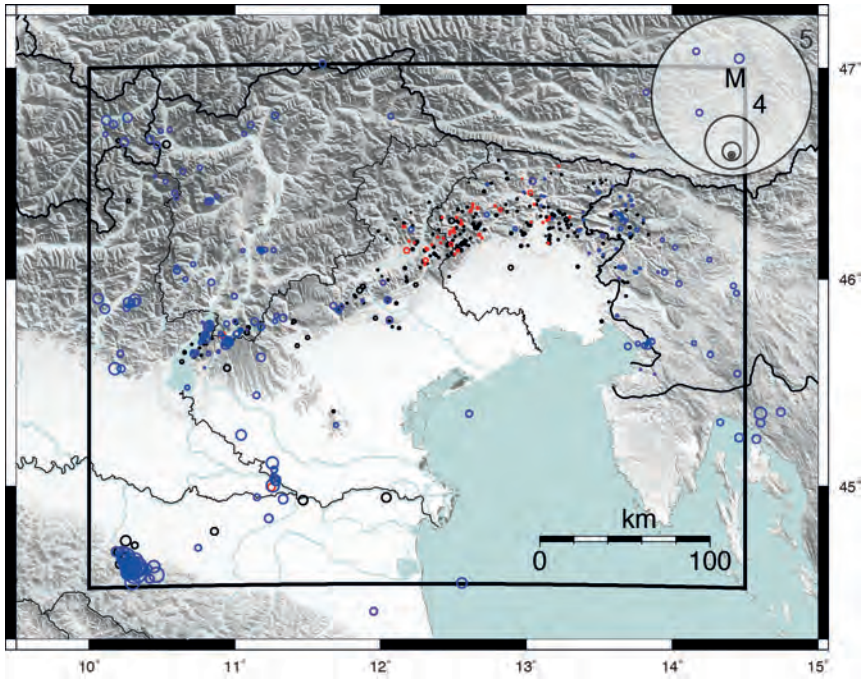

Fig. 4 - The earthquakes of 2011 NEI bulletin that Antelope® lost in the validation procedure (black circles) and during the stress tests done without short-period network (red circles) and extra-OGS stations (blue circles).

4. Conclusions

The aim of this study is the tuning of the Antelope® parameters for the real-time automatic locations in NE Italy. These locations are performed by the Antelope® software package and they are crucial for the civil defense organizations of three Italian regions (FVG, Veneto and Trentino) that coordinate contingent emergency activities. If compared with the starting model, our new parameters generate a strong increment in the number of recognized events and their related locations give a final MDE value which is consistent with the uncertainties associated to the NEI bulletin; these results are confirmed and improved in the validation task performed on the 2011 data. It is important to underline that we are looking at automatic (and not manually revised) locations and consequently in some cases the efficacity of the results could seem not very satisfactory if compared with the manual revised data.

Other relevant conclusions are:

- the detection parameters are very important to recognize the seismic events and to discriminate between local, regional, and teleseismic earthquakes; in particular, the frequency ranges for filtering the signals and the grids definition are tunings strictly connected and crucial for all the subsequent procedures. The system must be capable of detecting as many events as possible, also in case of earthquakes occurring with a few seconds between each other. The SNR ratio can be inefficient in this case, because the earthquakes can overlap each other in the STA/LTA computation. However, our configuration of parameters 'det_tmin' and 'det_tmax' seems to work satisfactorily, as demonstrated by the double events (M_L=2.8 and M_L=3.8) occurring on February 12, 2013

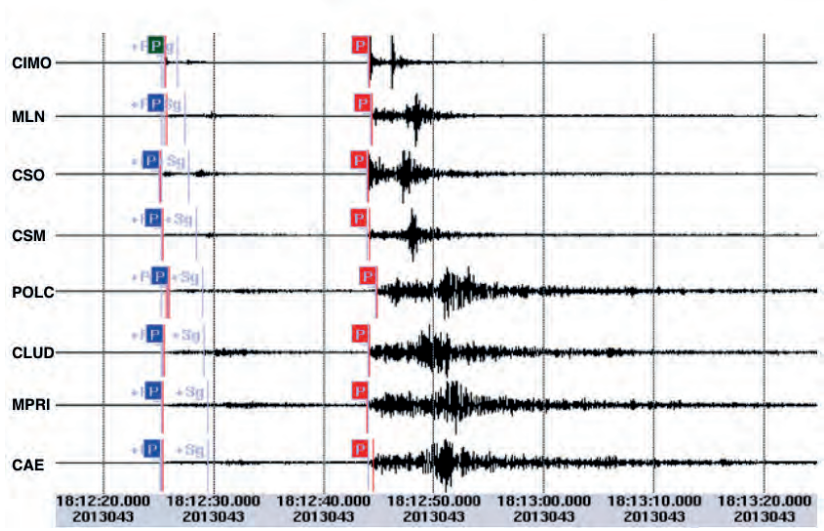

Fig. 5 - The detection and the related association of P phases (manually revised) for the double events occurred on February 12, 2013 within 19 seconds from each other at the border between FVG and Veneto (the locations are almost the same). The second event (M_L=3.8 with P phases in red) is larger than the first earthquake (M_L=2.8 with P phases in blue/green); the stations codes are reported in Tables 1 and 2.

within 19 seconds between each other at the border between FVG and Veneto regions and correctly detected and located by Antelope® (Fig. 5);

- the geographic distribution of the recording stations is irregular: high density characterizes the pre-Alpine sector of FVG region (the interstation distance is 10 km), while a lower density can be found in the Veneto plain (the interstation distance can reach 50 km). This network configuration influences strongly the events recognition and, therefore, the magnitude completeness in several areas. The selection of a minimum number of stations as function of maximum source-receiver distance has a consistent improvement in the percentage of recognized earthquakes. At the same time, this irregular spatial distribution of the recording stations makes the adoption unsuitable of any type of weights in the grid association, because the accuracy of the locations worsens strongly, especially in case of earthquakes occurring at the border of the NEI area;
- the GENLOC algorithm performs inversion starting from a location done by the grid associator; the GENLOC searches a local minimum close to the starting location but, if it is totally wrong, the inversion cannot adjust this result. The adoption of a local velocity model improves the accuracy of the locations and reduces the related uncertainties;
- in the automatic location we associate only the P phases but not the S phases, because they are difficult to pick and their propagation, particularly in the Po Plain, is very complex (Bragato *et al.*, 2011b);
- we performed also two stress tests that verify successfully the robustness of the system if a hypothetic broadcast crash causes the unavailability of some recordings.

The parameters obtained in this study have been operating on the automatic real-time Antelope® system since 2012 and the locations are published and continuously updated on the CRS web site (http://rts.crs.inogs.it). The system was also working during the Emilia sequence and the two mainshocks on May 20 and 29, 2012 were accurately located within 30 s from

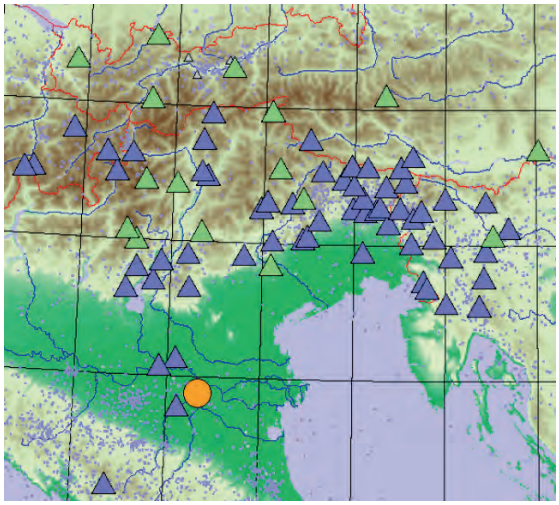

Fig. 6 - The location of the Emilia mainshock occurred on May 20, 2012 at 02:03; the orange circle shows the epicentre while the triangles indicate the recording stations that are associated (blue triangles), re-associated (green triangles) and not associated (orange triangles). The automatic location of the May 20 earthquake was lat=44.8904°N lon=11.2218°E (with an epicentral difference of 1.3 km from the INGV location) while it was lat=44.8501°N lon=11.0625°E in the May 29 event (with an epicentral difference of 1.8 km from the INGV location); the events are automatically located within 30 seconds from the earthquakes occurrence. The INGV locations are retrieved from ISIDe Working Group (2010).

the earthquakes occurrence (Fig. 6); in the first month after the mainshocks more than 800 earthquakes with $M_L \geq 2.0$ were automatically located.

The real-time Antelope® locations should be tuned with a specific configuration in order to obtain satisfactory performances and reliable results in a defined geographical area. With this issue our optimization procedure can be applied everywhere in accordance with the characteristics of the recording networks and the peculiarities of the local seismicity.

Acknowledgments. We acknowledge two reviewers, F. Vernon and N. Horn, for their constructive comments, which helped in improving this paper. We are grateful to the technical staff of the OGS Centro di Ricerche Sismologiche (CRS) for their efforts in the management with the information technology infrastructures and in the maintenance of the stations. The Rete Sismometrica del Friuli Venezia Giulia is managed by OGS with the financial contribution of the Regione Autonoma Friuli Venezia Giulia. The Rete Sismometrica del Veneto is managed by OGS with the financial contribution of the Regione Veneto. The waveforms are processed using Antelope® software (BRTT); the maps were produced using GMT software (Wessell and Smith, 1991) and Antelope® software (BRTT).

REFERENCES

Basili R., Valensise G., Vannoli P., Burrato P., Fracassi U., Mariano S., Tiberti M.M. and Boschi E.; 2008: *The Database of Individual Seismogenic Sources (DISS), version 3: summarizing 20 years of research on Italy's earthquake geology.* Tectonophys., **453**, 20-43.

Bianco F., Del Pezzo E., Castellano M., Ibanez J. and Di Luccio F.; 2002: *Separation of intrinsic and scattering seismic attenuation in the Southern Apennine zone, Italy.* Geophys. J. Int., **150**, 10-22.

Bragato P.L., Di Bartolomeo P., Pesaresi D., Plasencia Linares M. and Saraò A.; 2011a: *Acquiring, archiving, analyzing and exchanging seismic data in real time at the Seismological Research Center of the OGS in Italy.* Ann. Geophys., **54**, 67-75.

Bragato P.L., Sugan M., Augliera P., Massa M., Vuan A. and Saraò A.; 2011b: *Moho reflection effects in the Po Plain (northern Italy) observed from instrumental and intensity data.* Bull. Seismol. Soc. Am., **101**, 2142-2152.

Bressan G.; 2005: *Modelli di velocita' 1D dell'Italia nord-orientale*. Internal Report 2005/20, CRS 5, Udine, Italy, 18 pp.

Carulli G.B. and Slejko D.; 2005: *The 1976 Friuli (NE Italy) earthquake*. Giornale Geol. Appl., **1**, 147-156.

DISS Working Group; 2010: *Database of Individual Seismogenic Sources (DISS), Version 3.1.1: a compilation of potential sources for earthquakes larger than M 5.5 in Italy and surrounding areas*. INGV, Roma, Italy, doi:10.6092/INGV.IT-DISS3.1.1.

Fantoni R. and Franciosi R.; 2010: *Tectono-sedimentary setting of the Po Plain and Adriatic foreland*. Rend. Fis. Acc. Lincei, **21**, S197-S209.

Garbin M. and Priolo E.; 2013: *Seismic event recognition in the Trentino area (Italy): performance analysis of a new semiautomatic system*. Seismol. Res. Lett., **84**, 65-74.

Geiger L.; 1910: *Herbestimmung bei erdbeden aus den ankunftzeitzen*. K. Gessel. Wiss. Goett, **4**, 331-339.

Gentili S., Sugan M., Peruzza L. and Schorlemmer D.; 2011: *Probabilistic completeness assessment of the past 30 years of seismic monitoring in north-eastern Italy*. Phys. Earth Planet. Inter., **186**, 81-96.

Gruppo di Lavoro MPS; 2004: *Redazione della mappa di pericolosità sismica prevista dall'Ordinanza PCM 3274 del 20 marzo 2003*. Rapporto Conclusivo per il Dipartimento della Protezione Civile, INGV, Milano-Roma, Italy, 65 pp. + 5 appendici.

ISIDe Working Group; 2010: *Italian seismological instrumental and parametric database*. <http://iside.rm.ingv.it>.

Kennett B.L.N.; 1991: *IASPEI 1991 seismological tables*. Bibliotech, Canberra, Australia, 167 pp.

Klein F.W.; 1978: *Hypocenter location program HYPOINVERSE. Part 1: user's guide to versions 1,2,3 and 4*. U.S. Geol. Surv., Open-File Report 78-694, 113 pp.

Lee W.H.K. and Lahr J.C.; 1975: *HYPO71 (revised): a computer program for determining hypocenter, magnitude and first motion pattern of local earthquakes*. U.S. Geol. Surv., Open file report, 75-311, Menlo Park, CA, USA, 113 pp.

Lee W.H.K. and Stewart S.W.; 1981: *Principles and applications of microearthquake networks*. In: Saltzman B. (ed), Adv. Geophys., Suppl. 2, Academic Press, New York, NY, USA, 293 pp.

Mayeda K., Koyanagi S., Hoshiba M., Aki K. and Zeng Y.; 1992: *A comparative study of scattering, intrinsic, and coda Q-1 for Hawaii, Long Valley and central California between 1.5 and 15 Hz*. J. Geophys. Res., **97**, 6643-6659.

Pavlis G.L., Vernon F., Harvey D. and Quinlan D.; 2004: *The GENeralized earthquake LOCation (GENLOC) package: an earthquake-location library*. Comput. Geosci., **30**, 1079-1091.

Priolo E., Barnaba C., Bernardi P., Bernardis G., Bragato P.L., Bressan G., Candido M., Cazzador E., Di Bartolomeo P., Durì G., Gentili S., Govoni A., Klinc P., Kravanja S., Laurenzano G., Lovisa L., Marotta P., Michelini A., Ponton F., Restivo A., Romanelli M., Snidarcig A., Urban S., Vuan A. and Zuliani D.; 2005: *Seismic monitoring in northeastern Italy: a ten-year experience*. Seismol. Res. Lett., **76**, 446-454.

Rovida A., Camassi R., Gasperini P. and Stucchi M. (a cura di); 2011: *CPTI11, la versione 2011 del Catalogo Parametrico dei Terremoti Italiani*. INGV, Milano-Bologna, Italy, 30 pp.

Sandron D.; 2011: *Historic (since the beginning of 20th century) and instrumental (since 1977) seismicity recorded in NE Italy: a synthesis. Preliminary report*. Rel. 2011/60, CRS 12 RISK, **47** pp.

Slejko D., Carulli G.B., Nicolich R., Rebez A., Zanferrari A., Cavallin A., Doglioni C., Carraro F., Castaldini D., Illiceto V., Semenza E. and Zanolla C.; 1989: *Seismotectonics of the eastern Southern-Alps: a review*. Boll. Geof. Teor. Appl., **31**, 109-136.

Wessell P. and Smith W.H.F.; 1991: *Free software helps map and display data*. EOS Trans AGU, **72**, 441-446, doi:10.1029/90EO00319.

Corresponding author: Luca Moratto
Istituto Nazionale di Oceanografia e di Geofisica Sperimentale (OGS)
Centro Ricerche Sismologiche
Via Treviso 55, Udine, Italy
Phone: +39 040 2140247; fax: +39 040 327307; e-mail: lmoratto@inogs.it